ble that magnetic discontinuities (Néel lines or vortex lines) in the zig-zag tips and cusps play an important role in the walls displacement. Theoretical and further experimental investigations are in progress. It is worth noticing that zig-zags with a modulated amplitude may be of interest for memory devices.

[1]I. L. Sanders, R. M. Jones, and A. J. Collins, J. Phys. D **10**, 2503 (1977).
[2]M. J. Freiser, IBM J. Res. Develp. **23**, 330 (1979).
[3]R. C. Taylor, IEEE Trans. Magn. **16**, 902 (1980).
[4]M. Labrune, S. Hamzaoui, and I. B. Puchalska, J. Magn. Magn. Mater. **27**, 323 (1982).
[5]M. Labrune, S. Hamzaoui, C. Battarel, I. B. Puchalska, and A. Hubert, J. Magn. Magn. Mater. (in press).
[6]L. A. Finzi and J. A. Hartmann, IEEE Trans. Magn. **4**, 662 (1968).
[7]C. Battarel, R. Morille, and A. Caplain, IEEE Trans. Magn. **19**, 1509 (1983).
[8]G. Suran, K. Ounadjela, J. Sztern, and C. Sella, J. Appl. Phys. **55**, 1757 (1984).

Mössbauer effect studies of $Nd_2Fe_{14}B$ and related melt-spun permanent magnet alloys

F. E. Pinkerton
Physics Department, General Motors Research Laboratories, Warren, Michigan 48090-9055
W. R. Dunham
Biophysics Research Division, Institute of Science and Technology, 2200 Bonisteel Boulevard, University of Michigan, Ann Arbor, Michigan 48109

(Received 2 July 1984; accepted for publication 18 September 1984)

We report for the first time the ^{57}Fe Mössbauer spectrum of the ternary phase $Nd_2Fe_{14}B$, a technologically important new compound which forms the basis for a new class of high performance light rare earth-iron permanent magnet materials. From single phase powders we deduce the hyperfine parameters of the iron sublattices in the $Nd_2Fe_{14}B$ structure. Spectra of high-energy product ribbons obtained by a rapid quench process confirm that these permanent magnet materials are comprised predominantly of the $Nd_2Fe_{14}B$ phase.

Rapidly quenched Nd-Fe-B alloys[1,2] can exhibit intrinsic coercivities and energy products as large as 20 kOe and 14 MGOe, respectively. Such properties rival those of $SmCo_5$ permanent magnets, and their realization in light rare earth-iron materials represents a scientifically and technologically important advance in high performance permanent magnets. The presence of boron is vital to the development of high coercivities: x-ray and neutron diffraction studies[3] show that the highest energy product alloys are comprised of a new, tetragonal $Nd_2Fe_{14}B$ phase.

This letter reports for the first time the ^{57}Fe Mössbauer spectrum of $Nd_2Fe_{14}B$ in both single phase ingot and melt-spun ribbon form. We extract hyperfine parameters for the iron sublattices in the $Nd_2Fe_{14}B$ crystal structure. Spectra of melt-spun ribbons show the transformation from the magnetically soft Nd_2Fe_{17} phase in a boron-free $Nd_{0.15}Fe_{0.85}$ alloy to the $Nd_2Fe_{14}B$ phase when 5 at. % boron is substituted for iron. A consistent picture emerges in which optimum magnetic properties are associated with the formation of the $Nd_2Fe_{14}B$ phase, which may be magnetically hardened by melt spinning.[1,2]

The ^{57}Fe absorbance spectrum[4] of a single phase powder sample of $Nd_2Fe_{14}B$ is shown in Fig. 1.[5] The data are indicated by the circles, whose size indicates the uncertainty in the measurement. The spectrum is evidently quite complex, but by and large the iron sites have hyperfine fields H_{int} near 30 T at room temperature, similar to that of pure iron.[4] For comparison, Fig. 2 is the spectrum of a melt-spun $Nd_{0.15}(Fe_{0.95}B_{0.05})_{0.85}$ alloy having optimum magnetics[6] (12 MGOe energy product): the two spectra are nearly identical except for some broadening of the absorption lines in the melt-spun material, which we attribute to the small size (~ 50 nm) of the crystallites in the ribbon.[2] The similarity in these spectra corroborates x-ray and neutron diffraction evidence that the high-energy products obtained in melt-spun alloys are associated with formation of the $Nd_2Fe_{14}B$ phase. There are no iron-bearing second phases present in the rib-

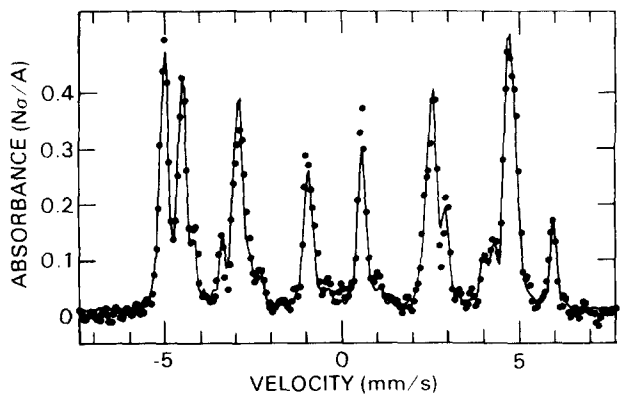

FIG. 1. Mössbauer absorbance spectrum of $Nd_2Fe_{14}B$ at room temperature. The solid curve is the fit to the spectrum using the parameters of Table I, and assuming Lorentzian lines with a full width half-maximum (FWHM) linewidth of 0.17 mm/s.

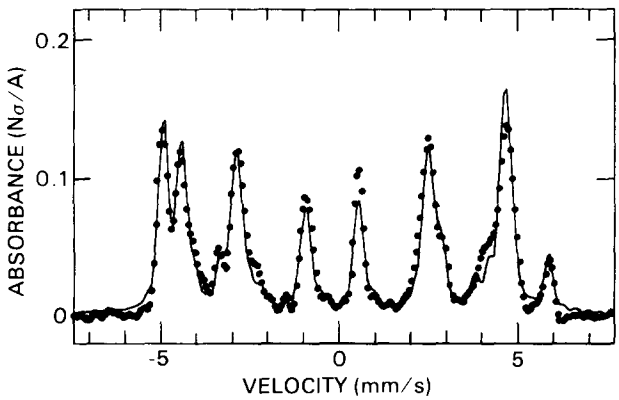

FIG. 2. Mössbauer absorbance spectrum of a $Nd_{0.15}(Fe_{0.95}B_{0.05})_{0.85}$ alloy melt spun at a substrate velocity of 15 m/s. The solid curve is the same fit as shown in Fig. 1, but with the FWHM linewidth broadened to 0.25 mm/s and the internal fields uniformly decreased by 2% to match the overall spread in the pattern.

bon within our detection limit ($\sim 5\%$); x-ray diffraction indicates that a small amount of free Nd is present.

Interpretation of the spectrum is guided by the crystal structure.[3] The $Nd_2Fe_{14}B$ structure has 68 atoms (four formula units) per unit cell. The 56 iron atoms are distributed on six crystallographically distinct sites, with the symmetries and occupancies listed in Table I. Starting with the relative sites intensities given by the site occupations in Table I, a computer fit to the $Nd_2Fe_{14}B$ spectrum was generated based on a six-site Hamiltonian including both magnetic and electric field gradient terms.[7] The fitting algorithm minimizes the root-mean-square error by quadratic interpolation in Fourier space. This computer program is a combination of the computer synthesis technique of Kundig[8] and our fast Fourier transform minimization techniques developed for fitting electron spin resonance data for free radicals.[9] The best fit, shown in Fig. 1, is nearly indistinguishable from the data. The corresponding hyperfine parameters are listed in Table I. Several key features of the spectrum are evident in Fig. 1. The intensity of the left most pair of peaks comes predominantly from the two most intense k sites, and the splitting graphically demonstrates that, although they are in crystallographically similar positions, the two k sites have quite distinct local environments. This is reflected in their hyperfine parameters in Table I. Furthermore, note that the right-most peak at 6 mm/s has no symmetric twin at -6 mm/s, indicating that this site has a substantial quadrupole

TABLE I. Room-temperature Mössbauer parameters for the six iron sublattices in $Nd_2Fe_{14}B$. Given are the site symmetry label, occupation number, isomer shift, internal field H_{int}, and quadrupole splitting $1/2\ eQV_{zz}$.

Site	Occupation	Isomer shift[a] (mm/s)	H_{int} (T)	$1/2\ eQV_{zz}$ (mm/s)
k	16	−0.20	29.9	0.03
k	16	−0.02	28.6	0.37
j	8	0.15	33.7	0.74
j	8	0.05	29.4	0.24
$\{^c_e\}$	4	−0.12	28.3	−0.91
	4	−0.06	26.1	0.19

[a] The isomer shift is measured relative to iron metal (NBS 1541) at 298 K.

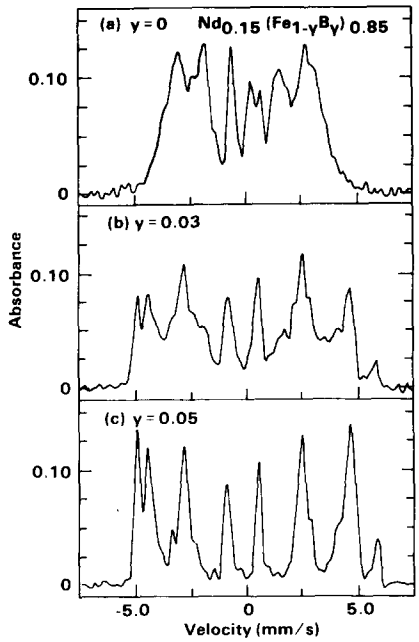

FIG. 3. Mössbauer absorbance spectra for a series of $Nd_{0.15}(Fe_{1-y}B_y)_{0.85}$ alloys melt spun at a substrate velocity of 15 m/s: (a) y = 0, (b) y = 0.03, and (c) y = 0.05.

splitting. This site, identifiable from its intensity as one of the j sites, is also distinguished as having the largest internal field (33.7 T) among the iron sites.

The spectrum of melt-spun $Nd_{0.15}(Fe_{0.95}B_{0.05})_{0.85}$ is fit in Fig. 2 using the *same* parameters generated from Fig. 1, by merely broadening the linewidth to 0.25 mm/s. A small ($\sim 2\%$) decrease in the internal fields was required to match the overall spread in the pattern. None of the Fe-bearing phases, Nd_2Fe_{17}, FeB, Fe_2B, or Fe metal, is detected in the spectrum. We note that in other samples (those with different cooling rates or stoichiometries) we are able to identify the Fe metal phase and the Nd_2Fe_{17} phase as components in our Mössbauer spectra. However, the 34 samples we have checked to date have at most the three phases (Fe, Nd_2Fe_{17}, and $Nd_2Fe_{14}B$) present in their Mössbauer spectra. Therefore, we feel that the spectra shown in this paper are diagnostic for the $Nd_2Fe_{14}B$ phase and that Mössbauer spectroscopy can be used to indicate the presence of this crystalline form.

Boron plays a crucial role in the magnetic hardening of Nd-Fe alloys: addition of only a few atomic percent boron can increase the maximum intrinsic coercivity by an order of magnitude as the material transforms to the $Nd_2Fe_{14}B$ phase.[1] This transformation is graphically illustrated in Fig. 3, which shows the room-temperature spectra for a series of alloys containing 15 at. % Nd, all melt spun at a substrate velocity of 15 m/s. The spectrum of the boron-free alloy (a) agrees well with the published spectrum of Nd_2Fe_{17},[10] the only stable binary Nd-Fe compound. The internal fields are modest (~ 16 T) primarily because the Nd_2Fe_{17} Curie temperature is only 330 K. The alloy is also magnetically relatively soft, with a maximum coercivity of less than 3 kOe. As boron is substituted for iron, the material transforms through a mixed-phase regime (b) to the high coercivity (17.5 kOe) $Nd_2Fe_{14}B$ phase (c). The mixed-phase spectrum demonstrates the stability of the $Nd_2Fe_{14}B$ phase: from the peak

intensities we deduce that this alloy consists of approximately 40% magnetically soft Nd_2Fe_{17} and 60% magnetically hard $Nd_2Fe_{14}B$, that is, all available boron is absorbed into the $Nd_2Fe_{14}B$ phase.

In conclusion, Mössbauer spectroscopy confirms that boron addition to Nd-Fe alloys promotes the formation of the ternary phase $Nd_2Fe_{14}B$, which can be magnetically hardened by melt spinning. We believe that this phase is the principal component in high-energy product rare earth-iron-boron materials prepared not only in our laboratory[1,2] but also by other investigators either by melt spinning [11–13] or powder metallurgy.[14] We have identified six iron sublattices, corresponding to the six distinct iron sites in the $Nd_2Fe_{14}B$ crystal structure.

We are grateful to Erwin Alson, Tom VanSteenkiste, and Neal Schaffel for technical assistance. We have benefited greatly from conversations with John Croat, Jan Herbst, and Robert Lee, and we thank John Smith and Frank Jamerson for their enthusiastic support.

[1]J. J. Croat, J. F. Herbst, R. W. Lee, and F. E. Pinkerton, Appl. Phys. Lett. **44,** 148 (1984).

[2]J. J. Croat, J. F. Herbst, R. W. Lee, and F. E. Pinkerton, J. Appl. Phys. **55,** 2078 (1984).

[3]J. F. Herbst, J. J. Croat, F. E. Pinkerton, and W. B. Yelon, Phys. Rev. B **29,** 4176 (1984).

[4]W. R. Dunham, C. T. Wu, R. M. Polichar, R. H. Sands, and L. J. Harding, Nucl. Instrum. Methods **145,** 537 (1977).

[5]The sample was confirmed to be single phase both by optical metallographic analysis of the starting ingot and by x-ray and neutron diffraction on the powder.

[6]Details of the melt-spinning process are given in Ref. 1. This sample was obtained at a melt-spinner substrate velocity of 15 m/s.

[7]The full Hamiltonian is given in Ref. 8. This fit assumes that the electric field gradient is parallel to the internal field, and that the electric field gradient tensor is symmetric. Each site can then be described solely in terms of its isomer shift, internal field H_{int}, and quadrupole splitting $eQV_{zz}/2$, where Q is the electric quadrupole moment and V_{zz} is the z component of the electric field gradient.

[8]W. Kunig, Nucl. Instrum. Methods **48,** 219 (1967).

[9]W. R. Dunham, J. A. Fee, L. J. Harding, and H. J. Grande, J. Magn. Reson. **40,** 351 (1980).

[10]V. K. Agarval and R. N. Kuz'min, Kristallografiya **16,** 774 (1971); Sov. Phys. Cryst. **16,** 670 (1972).

[11]N. C. Koon and B. N. Das, J. Appl. Phys. **55,** 2063 (1984).

[12]G. C. Hadjipanayis, R. C. Hazelton, and K. R. Lawless, J. Appl. Phys. **55,** 2073 (1984).

[13]D. J. Sellmyer, A. Ahmed, G. Muench, and G. C. Hadjipanayis, J. Appl. Phys. **55,** 2088 (1984).

[14]M. Sagawa, S. Fujimura, M. Togawa, H. Yamamoto, and Y. Matsuura, J. Appl. Phys. **55,** 2083 (1984).